JOINT EUROPEAN TORUS JET

JET–P(87)18

M. Bures, H. Brinkschulte, J. Jacquinot, K.D. Lawson, A. Kaye
and J.A. Tagle

The Modification of the Plasma Edge and Impurity Production by Antenna Phasing during ICRF Heatingon JET

The Modification of the Plasma Edge and Impurity Production by Antenna Phasing during ICRF Heatingon JET

M. Bures, H. Brinkschulte, J. Jacquinot, K.D. Lawson, A. Kaye
and J.A. Tagle

JET-Joint Undertaking, Culham Science Centre, OX14 3DB, Abingdon, UK

Preprint of Paper to be submitted for publication in
Plasma Physics and Controlled Fusion

Abstract

During RF experiments on JET a strong modification of the plasma edge is generally observed. Density and temperature profiles in the scrape-off layer usually flatten and enhanced impurity and neutral influx is observed. Metallic impurity influx originating from the antennae screens is also observed. This is especially true when the antennae are phased so that the excited spectrum contains a large fraction of power in the waves with $k_{//} = 0\text{-}2\ m^{-1}$. A radially localized enhancement of the particle diffusivity $D_{\perp}(a)$ across the plasma edge results. When the antennae are phased in the quadrupole configuration with the maximum power emitted at $k_{//} = 7\ m^{-1}$ a strong modification of the edge is not observed. The scrape-off layer profiles scale as in the ohmic discharges. Then both the light and metal impurity influxes become substantially reduced.

1. Introduction

One of the important problems associated with ICRF heating of tokamaks is the impurity release and the corresponding uncontrolled density increase during the RF pulse. Usually it is observed that the plasma edge and the scrape-off layer (SOL) become modified. It is believed that both the impurity release and the enhanced recycling are correlated with the plasma edge modification. Sputtering from the limiters by the hydrogen and impurity ions accelerated in the sheath potentials, charge exchange sputtering of the structures and the vessel wall are often suggested as the main causes of the impurity release. The contribution to the impurity sputtering by the fast ion population created by the RF and the role of the density and field fluctuations in the plasma edge are not yet conclusively assessed. There was a large number of studies performed on different machines trying to elucidate the processes responsible for the RF impurity production.

On the TFR [TFR Group 1985a; TFR Group 1985 b)] the influence of the $k_{//}$ shaping on the impurity production and heating efficiency was investigated. It was concluded that the rate of oxygen production at the onset of RF is reduced when the $k_{//} = 0$ is not excited. The evolution of the SOL profiles was not correlated to the energy balance of the bulk plasma. The hydrogen and impurity influxes, however, always increase. On the contrary it was reported [Noda et al., 1984] that during the ICRF heating on the JIPP-IIU tokamak the hydrogen and deuterium influxes from the limiter decrease while the carbon and oxygen influxes substantially increase. The Faraday shield of the antenna becomes less important as the impurity source. The oxygen influx from the graphite limiters limited the the RF power which could be coupled without disrupting the plasma. The decrease of edge recycling during the RF heating pulse was also observed on the TEXT tokamak when the pump limiter ALT-I was biased negatively [Conn et al, 1986]. A strong modification of the SOL density profiles was observed during the Alfve'n wave heating on TCA tokamak [A de Chambrier et al, 1984]. The electron density was observed to decrease in proportion to the applied RF power and nearly flat profiles were obtained. It was suggested that the antenna acts as a large Langmuir probe biased by the oscillating antenna voltage and drawing alternatively the electron and ion current. The resulting particle interaction with the antenna surface becomes an efficient mechanism for the impurity sputtering. An important reduction of the radiated power increase during the RF heating was observed in JFT - 2M tokamak when the excited $k_{//}$ spectrum was modified by the antenna phasing [M. Morietal 1985, H. Tamai et al 1987]. The most favourable results were obtained when three antennae were driven out of phase. The peak power was then radiated approximately at $k_{//} = 8m^{-1}$. The heavy impurity influxes were also strongly reduced.

The existence of the fast ions with energies $> 10^5$ eV in the SOL of PLT was demonstrated during the H^+ minority and first H^+ harmonic heating regime [Manos et al, 1984]. However, the importance of the fast ions for the impurity production was not assessed quantitatively.
One mechanism suggested as responsible for the enhanced particle loss during the RF is the formation of a quasistationary potential in the plasma with an associated electric field. The resulting cross field flux of particles striking the wall, limiters and screen can be considered to

be a source of the RF induced impurities. On Macrotor [Taylor et al, 1983] it was suggested that the electrons are driven into the antenna, producing a radial electric field at the plasma edge which then pumps the plasma out. The build-up of the edge potential as a result of the non linear interaction of ions with the oscillating radial electric field was suggested in Ref. [Grigor'eva et al, 1984]. In both cases the density clamping was observed resulting from the increased particle losses. A similar mechanism, the sputtering induced by the ions accelerated by the electric field near the antenna was suggested to be responsible for the metal release from the antenna screen during thê ICRF heating in JFT-2M tokamak [Ogawa et al, 1987]. From these experiments follows that the metal impurities released near the antenna could be explained by such a mechanism. On the other hand the light impurities such as carbon and oxygen are sputtered from limiter by the ions accelerated in the sheath potential. No difference between high and low field side excitation was observed. The estimates of the perpendicualar ion energies associated with the oscillating electric field in the vicinity of antenna in large devices indicate that the ion sputtering can become important at high RF power levels [Itoh et al, 1984]. In this paper we present evidence for enhanced particle diffusion across the plasma edge during the RF and show correlation of this mechanism with the excited RF spectrum. A correlation with the impurity production is also demonstrated. The general trends of the impurity behaviour during the ICRF heating on JET was treated in Refs. [Denne et al 1985, The JET Team 1986, Behringer et al 1986].

2. Experimental arrangement

In JET, three antennae have been operated since the summer of 1985 [Jacquinot et al 1986, Lallia 1986, Kaye 1985]. Two are of the dipole/quadrupole type. The third antenna located 180° opposite in the torus is of the monopole/dipole type. The dipole/quadrupole antenna consists of four conductors which can be internally phased so as to excite a $k_{//}$ spectrum which emits the maximum of RF power at $k_{//} = 0m^{-1}$. For higher $k_{//}$ the radiated power is monotonically decreasing. In the quadrupole phasing there is no power radiated at $k_{//} = 0m^{-1}$ and the launched spectrum is peaked at $k_{//} = 7m^{-1}$. The monopole/dipole antenna consists of two conductors. When powered in phase the monopole configuration excites a spectrum peaked at $k_{//} = 0m^{-1}$. For increasing $k_{//}$ the radiated power decreases as in the dipole case. When integrated over the whole spectrum of $k_{//}$ the resulting coupling resistance of the monopole antenna is typically twice the resistance of the dipole. For the details see Refs [Jacquinot et al 1986, Kaye 1985]. In addition, these antennae which were installed side by side, can be mutually locked in phase. Therefore a variety of $k_{//}$ spectra can be excited. When the two dipoles are driven 180° out of phase a spectrum emitting a peak power at $k_{//} = 2$ and $6\ m^{-1}$ is excited as shown in Fig.1 together with the spectrum for quadrupole. A small degree of directivity ≈ 5% can also be produced with the antennae 90° out of phase [Bhatnagar et al, 1986]. The peak of radiation resistance at $k_{//} = 0m^{-1}$ for the two out of phase dipoles is due to the coaxial modes. These waves are propagating in the region between plasma surface and the wall. They are excited by the radial currents of the conductor feeders. It should be mentioned, however, that until now no experimental evidence was presented supporting existence of these waves in the boundary layer. In fact to obtain a good agreement between the theory and the experimental results with regard to the coupling resistance, coaxial modes have to be excluded from the model. The various phasing conditions were compared using a target plasma of low density $\langle n_e \rangle \tilde{=} 1.1 \times 10^{19}\ m^{-3}$ to maximise the impurity production. The mutual phasing of two dipoles at 0°, ± 60°, ± 90°, ± 180° did not produce any important differences in either the impurity release, modification of plasma edge or heating effects. In contrast the internal quadrupole phasing, resulted in a very different behaviour of the plasma edge as compared with that observed with the dipole configuration. The impurity release and recycling was greatly modified as was, to a lesser

degree, also the heating efficiency. The specific plasma behaviour in both these cases will be described in the next Sections. The third antenna in the monopole phasing was used to monitor the coupling resistance which can be considered to be a measure of the edge density.

A very low power is applied to this antenna during the experiments in order not to perturb the plasma edge. Fig. 2 shows the theoretical antenna radiation resistance as a function of the density profile parameters and in particular a strong dependence on the edge density n(a) should be noticed A code [Evrard et al, 1986], based on a single pass model, was used to calculate the radiation resistance. The density profile in the plasma is defined as $n(x) = n(a) + [n(0) - n(a)] \times (1-r^2/a^2)^{\alpha}$. In the SOL the exponential decay is assumed, i.e., $n(x)_{SOL} = n_{MIN} + [n(a) - n_{MIN}] \exp - (x-a)/\lambda$. Here n_{MIN} is chosen to avoid the lower hybrid resonance in front of the screen. The peaking of the profile and the characteristic scale length of the density decay in the SOL are less important. This applies at a given excitation frequency, magnetic field, configuraton of the antenna and distance between the antenna screen and plasma edge. The experiments were performed in a deuterium plasma with hydrogen gas as a minority. The toroidal field was typically 2.2T and the operating frequency such as to place the minority cyclotron layer at the centre of the plasma. No carbonisation of the vessel was performed during the two months before the experiment.

To elucidate the behaviour of the SOL two Langmuir probes were installed in the protection tile of one of the antennae [Brinkschulte et al, 1986] as shown in Fig. 3. These enable us to obtain a measurement of the plasma density and the electron temperature at two radii 38 times during the discharge. In the present experiments the two probes are positioned within the SOL at 15 and 27 mm from the plasma edge. The description of the probes and the first results obtained during the RF have been reported earlier [Brinkschulte et al, 1986, Erents al, 1986a)]. Another set of Langmuir probes is installed in JET measuring plasma profiles close to the wall at the top of the vacuum vessel. There is satisfactory agreement between the data obtained with this set of probes and the "antenna" probes. The results for the ohmic discharges obtained by the probes at the top of the vacuum vessel were reported in Ref. [Erents et al, 1986b].

3. Experimental results

To demonstrate the effect of antenna phasing on the plasma behaviour discharges with the target plasma in nearly identical conditions were selected. The RF total power coupled into the plasma with dipoles was typically in the range of ≈ 1.7 MW. In the quadrupole configuraton, the power was limited by antenna arcing and at best 1.35 MW was coupled. The radiation resistance is typically 0.7 - 1 Ω. This figure includes the resistance of the transmission line and the antenna screen ($R_L \approx 0.5$ Ω). The coupling resistance of dipoles is typically 4-6 Ω depending on the plasma density at the instant of the application of RF power. For the same power delivered to the plasma the resulting voltages on the antenna and transmission lines are much higher in the quadrupole case and this is the main factor limiting the coupled power. The quadrupole phasing exhibits a number of beneficial features as compared to the dipoles. The most important results are summarised in Table I. $\Delta[ICrXXI/\langle n_e \rangle]/P_{RF}$ is the RF induced increase of the CrXXI line radiance normalized to the volume averaged density and RF power. $\Delta P_{rad}/P_{rf}$, $\Delta Zeff/P_{RF}$ and $\Delta \int n_e d\ell/P_{RF}$ are normalized increases of radiated power effective charge and the line integrated density. $\Delta \sum \phi_D^{TOT}/P_{RF}$ is normalized total neutral influx from the limiters and the wall. τ_{INC} is the incremental confinement time of the additional energy measured from the energy evolution. In turn, the energy time evolution was obtained from the MHD equilibrium code as well as from the density and temperature profiles. The results can be stated as follows:

For quadrupoles,

- the increase of the intensities of the metal lines CrXXI and NiXXV normalized to the plasma density and the RF power is substantially lower. Note that the line radiance normalized to the plasma density is a rough measure of the number of metallic ions along the line of sight.

- the increase in the power radiated by the plasma is reduced despite a larger increase in density. In fact the ratio P_{rad}/P_{input} remains practically constant during the ohmic and RF phases.

- the increase in the line-averaged density (measured at the central chord of the plasma) is larger and also

- the neutral deuterium influx ϕ_D from the limiter and wall becomes much higher.

In terms of the heating efficiency defined by the incremental confinement time $\tau_{INC} = \Delta W/\Delta P$, the quadrupole appears to perform better, typically by 25%.

The traces of Fig. 4a) show the time evolution of the CrXXI line which is observed at 149.89 Å and the NiXXV line observed at 117.94 Å. One antenna which was powered has a nickel screen while the second has a screen coated by chromium. Only the screen of the powered antenna releases the corresponding metal impurities as discussed in Section 6. Both nickel and chromium intensities are much higher during the dipole phasing. When the measured values during the RF are properly normalized the results indicate that the number of metallic ions observed in the plasma during the RF are much lower when the antennae are phased as quadrupoles. The same conclusions can be drawn from the intensity evolution of the CrXXII and NiXXVI lines. The NiXXVI and CrXXII lines are observed at 165.35 and 223.01 Å, respectively. In contrast the CrI line intensities measured at 4254.35 Å do not show the similar behaviour, as shown in Fig. 4b. It should be noticed, however, that the CrI signals might contain large fractions of the continuum radiation and should be interpreted with care. The consequences of a somewhat different behaviour of the low and high ionisation stages of the chromium for the interpretation of the edge behaviour are discussed in sections 6 and 7.

Fig. 5 shows the time evolution of a number of the plasma parameters in the two cases. It is observed that the carbon influx from the wall is 2-3 times higher with the dipoles, while the neutral influx from the limiter actually decreases during the RF pulse. Thus the results suggest that the plasma edge behaviour is quite different in the two cases. It should be noted here that the evolution of the neutral influxes from the wall and limiter do not reflect the exact time evolution at the onset of the RF power. Due to the computer processing of the measured signals to obtain the absolute neutral influxes from the H_α measurements, the detailed information about the time evolution is lost. In fact the evolution of the directly measured signals is very similar to that of the carbon trace in Fig. 5. The uncalibrated signals always show the modulation by the sawteeth activity. The amplitude of this modulation depends on the plasma parameters and particularly on the amount of coupled RF power.

4. Probe measurements in the SOL

The electron plasma density and the electron temperature SOL profiles obtained by the antenna Langmuir probes are presented in Figs. 6a) and 6b). The profiles are compared in the ohmic and the RF equilibrium phase. Both density and temperature are extrapolated to the last closed magnetic surface under the assumption that the profiles decay exponentially. This is in accordance with a model where the parallel particle and energy transport in the SOL dominates the perpendicular transport. Because the profiles are inferred from only two radial measurements together with an assumption based on a model, they should be interpreted with care. Recent correlation with the data obtained from the set of probes placed at the top of the vacuum vessel, where more radial measurements are used to reconstruct the profiles, suggests that the density and temperature profiles in the SOL exhibit indeed the exponential decay. The dipole profiles exhibit a behaviour already observed earlier [Brinkschulte et al, 1986, Erents et al, 1986a]. Both the density and temperature profiles flatten. It will be shown later that the density profile flattening is correlated to the changes of the coupling resistance.

In contrast, this edge modification is not observed with the quadrupole phasing. The profiles do not flatten and both the density and temperature increase everywhere in response to the increase of the total number of particles in the plasma volume and the higher total power input. To check whether this behaviour extends to higher densities a partial density scan was performed with the quadrupole phasing. The density was raised from $\langle n_e \rangle = 1.1 \times 10^{19}\ m^{-3}$ to $1.75 \times 10^{19}\ m^{-3}$ in four steps. Figs. 7a) and 7b) show the profiles for the lowest and highest density. Both the ohmic and RF profiles show the same dependence, that is the edge density increases with the higher plasma density while the temperature is correspondingly lower. No flattening is observed during the RF. The RF power coupled to the plasma in both cases was essentially the same.

5. Correlation of the edge beahviour and the coupling resistance

It was observed very early during the ICRH experiments on JET that the plasma edge is modified during the RF pulse [Bures et al, 1985]. This follows since the plasma density increase during the RF pulse is not reflected in an increase in the coupling resistance. Under certain conditions, especially after the carbonisation, the density increase can be as high as 70%. Consequently unless there is a peaking of the density profile and an improved particle containement the edge plasma density should increase correspondingly as should the coupling resistance. It has been observed that the coupling resistance is a function of the density measured just before the application of the RF. Its increase is typically $\approx 1\ \Omega$ for monopole and $0.7\ \Omega$ for dipole per $10^{19}\ m^{-2}$ of the line density (measured at the central chord). During RF heating the density profile always broadens. Fig. 8 shows the evolution of the line density of two radii. The first is measured along the vertical chord crossing the plasma centre while the second along a vertical cord roughly 20 cm from the edge. The resulting broadening of the density profile during the RF is represented by a decreasing peaking factor α, as described in Section 2.

The time evolution of the edge density obtained by the Langmuir probes is presented in Fig. 9. We observe that in the quadrupole case the edge density increase follows the mean density increase shown in Figs. 5 and 8. In contrast the edge density becomes depleted during the dipole pulse. This depletion has to be confined to the outermost region of the plasma, because at a distance of 20 cm from the antenna the density is still increasing. Thus the mechanism which depletes the edge density in the dipole phasing has to be localized. In Fig. 10 the coupling resistance of the dipole antenna is shown for the same shot. A clear correlation with the edge density time evolution should be noted. The full RF power is usually applied after 200 msec of a low power pedestal which allows locking of the phase and frequency loops so that the RF generators can be operated correctly. The drop of the coupling resistance upon the application of the full RF power indicates the corresponding drop in the edge density. It was observed that this

mechanism comes into operation already at very low powers, that is $\geq$ 100 kW. For the case of the quadrupole phasing the corresponding coupling resistance measurement is not available. This is due to the fixed tuning stubs being installed on the transmission lines close to the antenna, this inhibiting the measurements. However, the third antenna, see Section 2, was operated during a few quadrupole shots in a diagnostic mode, at a low power level, typically $\approx$ 50 kW. The edge behaviour is nevertheless expected to be dominated by the quadrupole antennae powered at the MW level. To demonstrate the remarkable correlation between the edge density increase measured by the Langmuir probes and the evolution of the coupling resistance measured by the third antenna, Fig. 11 shows a discharge where the power delivered by the quadrupoles was not constant due to the generator tripping. Thus the edge density becomes correlated to the power and correspondingly to the coupling resistance of the antenna in diagnostic mode.

6. Discussion of results

A number of conclusions can be drawn from the results presented here.

- First consider the modification of the profiles in the SOL during the RF with dipole phasing. Disregarding the ionisation of neutrals close to the wall based on the fact that the mean free ionisation path of the neutrals becomes much larger than the radial dimension of the SOL, the flattening of the density profile corresponds to the increase in the particle diffusion across the plasma boundary. The corresponding decrease of the edge density n(a) is correlated with the decrease of coupling resistance. The behaviour of the coupling resistance, which is primarily a measure of the edge density n(a), supports the straightforward extrapolation of the density over the last 15 mm from the probe 1 to the plasma edge. We assume a model where the total number of particles per second flowing across the plasma surface S is equal to the total number of particles reaching the limiter by a parallel flow within the SOL.

- A simple expression for the diffusion coefficient becomes $D_{\perp}(a) = v_s(a)\lambda_I \langle\lambda_n\rangle/L_{//}$. The expression follows from the argument that the total particle flux across the last closed magnetic surface equals the parallel flux in the SOL. Thus $D_{\perp}\langle\frac{dn}{dx}\rangle_a S = n(a)v_s(a)\lambda_I L_p$. Here $v_s(a) = [k(T_e+T_i)/m_i]^{\frac{1}{2}}$ is the sound speed, λ_I is the e-folding length of the particle flux measured at the limiter and $\langle\lambda_n\rangle \tilde{=} (1.5 - 2.0)\lambda_n$ is the average e-folding lenght of density taking into account the poloidal inhomogeneity of the SOL. λ_n is obtained from the probe measurements and $L_{//} = S/L_p$ is the equivalent connection length. L_p is the total effective limiter length (in the poloidal direction) exposed to the parallel particle flux. In the ohmic phase the diffusion coefficient is found to be $D_{\perp}(a) \tilde{=} 0.5 - 1 m^2 s^{-1}$, while during the RF it can increase in the case of low current, low density operation by a factor 5-10. Thus both the probe and coupling resistance measurements indicate a density depletion at the plasma edge which can be characterized by a radially localized increase in diffusion over a thickness smaller than 15 cm. It is predominantly the increase of the e-folding length of the density and particle flux radial decay which indicate the change in diffusion coefficient $D_{\perp}$.

The sound speed and the equivalent connection length change only slightly. The edge density does not respond to the global density increase which, as previously mentioned, can be detected very close ($\approx$ 20 cm) to the plasma edge as shown in Fig. 8. During the quadrupole phasing no flattening of the scrape-off profiles is observed. Consequently the edge density responds to the increase of total number of particles and is measured both by the probes and the coupling resistance measurements. The estimates of the particle flux from the probe results agree with the H_α measurements within the factor 2 - 2.5 and also with the edge density calculated from the particle balance at the edge given by $n(a) = \Sigma\Phi a\langle\lambda_n\rangle/2VD_\perp(a)$. Here $\Sigma\Phi$ is the total neutral influx, V the plasma volume and a is the minor radius. The parallel energy flux within the SOL is consistent with conducted power into the SOL (obtained from the total power input and the radiated power) within a factor of 2.

Consider the particle balance in the region of the enhanced diffusion between radii x_2 and a as shown in Fig.12. The outflux of particles across the plasma surface S(a) at the radius a is equal to the influx of particles across the surface $S(x_2)$ and the total number of ionisations per second S_i within the volume $2\pi^2R(a^2-x_2^2)$. Thus $\Gamma(a) = \Gamma(x_2)x_2/a + S_i/4\pi^2Ra$ where the local flux is $\Gamma(x) = D_\perp(x)dn(x)/dx$. During the dipole operation the density gradient $dn(x_2)/dx$ increases which implies that for the same outflux $\Gamma(a)$ the number of ionisations S_i has to decrease. This is consistent with the increased mean free path of ionisation of neutrals due to the lower edge temperature and density.

- With respect to the metal impurities released during the RF it was reported earlier [Behringer et al, 1986] that the antenna screens are the main sources of the nickel and chromium influxes during the RF. To a lesser degree there is also a contribution to the fluxes from the limiters. To release the metal from the screen the antenna has to be activated. When the two adjacent antennae are not activated at the same time, no metal influx is observed from the screen in front of the inactive antenna. Remarkably, even high powers applied to the adjacent antenna do not imply any substantial metal release from the second antenna screen. A typical example of these effects can be seen in Fig.13. Thus the following conclusions can be drawn:

- The increase of the parallel energy flux within the SOL during the RF is responsible for the neutral and the impurity influx increase from the limiters and wall. The release of the metal from the antenna screen is not caused by this increase of the parallel energy flux. Thus it has to be caused by a perpendicular particle and energy flux.

This mechanism is localized and toroidally does not extend much beyond the antenna. From that follows that the release mechanism is likely to be correlated to the RF field pattern which, in JET, is localized to the volume of the cone defined by the surface of the antenna and the focalization of the field in the radial direction. The fact that the CrI line intensity does not substantially differ during the dipole and quadrupole phasing suggests that the number of metal atoms released from the screen is similar. However, the number of the ions reaching the plasma centre becomes substantially reduced when the antennae are phased as quadrupoles. This is due to the more efficient screening which results from the more favourable temperature and density profiles in the SOL and the plasma edge.

- Considering the behaviour of the neutral influxes during the dipole phasing it was consistently observed, in the present range of plasma parameters, that the limiter neutral flux becomes somewhat lower at the end of the RF pulse than in the ohmic phase. Because it is unlikely that the particle confinement would increase during the RF, the electron density increase has to be explained by the additional influx of light impurities such as carbon and oxygen. The very important increase of carbon influx is indeed observed. To which extent the influxes from the antennae contribute to the total influxes cannot be assessed quantitavely because the corresponding measurements on the antennae are not available.

- An alternative explanation to the observed changes of the SOL density profiles was suggested in Ref. [Erents et al, 1986a]. Increased ionisation in the SOL due to the temperature increase and the corresponding change of the particle source function was shown to be consistent with the density rise. However, it is difficult to explain the observed different behaviour of coupling resistance during the dipole and quadrupole phasing in terms of this mechanism. While the increased ionisation in the SOL contributes to the evolution of the profiles in both cases, it has to be concluded that in the dipole phasing and the present plasma parameter range, the locally enhanced diffusion has to dominate the behaviour of the plasma edge. Indeed, the average level of the coupling resistance is very seldom seen to increase during the RF pulse.

7. Conclusions

An important difference in the plasma edge modification by the RF field was observed between dipole and quadrupole phasing of the antennae in JET. When the antennae are phased as dipoles a very strong modification of the plasma edge is observed. The electron density at the last closed magnetic surface becomes depleted. This depletion becomes localised to a region a-r < 20 cm and can be characterized in terms of the locally enhanced particle diffusion $D_{\perp}(a)$ across the plasma edge. Although we do not have at present any experimental evidence, we believe that the formation of the quasi-stationary potential field near the antenna is responsible for the density depletion at the edge. In contrast the edge does not become modified in the quadrupole phasing. The edge density increases in response to the density increase caused by the higher power input into the vessel. The metal influx from the screen is then considerably reduced. There are two possible explanations for the difference in the chromium and nickel influx during the dipole and quadrupole phasing. First the edge density depletion and the sputtering of the screen are correlated. In dipole case, the resulting perpendicular particle and energy flux results in metal sputtering from the antenna screen. The phenomenon responsible for these effects becomes localized close to the antenna and consequently can be correlated with the spatial extent of the RF field. The localized density depletion is quickly redistributed along the magnetic field. In the second explanation the amount of the metal atoms released from the screen is considered to be same in both cases of the phasing as is suggested by the evolution of the CrI line intensity. However due to the absence of the edge modification (decreased density and temperature) with the quadrupoles, the atoms released from the screen become ionised in the SOL and are prevented to enter the plasma. The results indicate that the absence of the partial waves close to $k_{//} = 0$ is the essential factor. The high voltages at the antenna with quadrupole phasing, due to the low coupling resistance, become of secondary importance.

Acknowledgements

The authors are indebted to Drs K Behringer, M Stamp, J Hammet, D Gambier and F Sand for the valuable discussions. We also wish to acknowledge the hard work of the JET team who build, operated and performed the measurements which made this study possible.

References

1. Behringer K. et al., Proc. 13th Europ. Conf. on Contr. Fusion and Plasma Physics, Schliersee (1986) Vol 10C, Part I, 180

2. Bhatnagar V.B. et al., Proc. 13th Europ. Conf. on Contr. Fusion and Plasma Phys. Vol 10C, Part II, p. 77, Schliersee (1986)

3. Brinkschulte H. et al, Proc. 13th Europ. Conf. on Contr. Fusion and Plasma Phys., Vol 10C, Part I, p. 403, Schliersee (1986)

4. Bures M. et al., Proc. 12th Europ. Conf. on Contr. Fusion and Plasma Phys., Vol 9F, part II, p. 148, Budapest (1985)

5. Conn R.W. et al., Proc. 11th IAEA Conf. on Plasma Phys. and Contr. Nuclear Fusion Res. (1986) IAEA-CN-47/A-N-6 (to be published).

6. de Chambrier A. et al., Journal of Nucl. Mat., 128 & 129 (1984) p.310.

7. Denne B. et al., Proc. 12th Europ. Conf. on Contr. Fusion and Plasma Phys. Budapest (1985) Vol 9F, Part I, 379

8. S.K. Erents et al, 7th Int. Conf. of Plasma Surface Interactions in Fusion Devices, Princeton 1986, to be published in Journal of Nucl. Materials

9. S.K. Erents et al, 1986, to be published in Nuclear Fusion

10. Evrard M.E. et al, Proc. 13th Europ. Conf. on Contr. Fusion and Plasma Phys., Vol 10C, Part II, p. 133, Schliersee (1986)

11. Grigor'eva L.I. et al, Journal of Nucl. Mat., 128 & 129 (1984) 317

12. Itoh S.I. et al., 7th Joint Varenna-Grenoble Symposium on Heating in Toroidal Plasma, Rome, C23 (1984)

13. Jacquinot J. et al., Plasma Phys. and Contr. Fusion Vol. 28 (1986) 1

14. The JET Team, Plasma Physics and Contr. Fusion, Vol. 28, Number 9A (1986) 1401

15. Kaye A.S. et al., Proc. of the 11th Symposium on Fusion Engineering, Austin, Texas, (1985) Vol II, p. 1204

16. Lallia P.P. et al., Plasma Phys. and Contr. Fusion, Vol. 28 (1986) 1211

17. Manos D.M. et al., Journal of Nucl.Mat., 129 (1984) p.319.

18. M. Mori et al, Proc. 10th IAEA Conf. on Contr. Fusion and Plasma Phys. (1984) IAEA-CN-44/F-I-3, p.445.

19. Noda N. et al., Journal of Nucl. Mat., 128 & 129 (1984) p.304.

20. Ogawa H. et al., Journal of Nucl. Mat., 128 & 129 (1984) 298

21. H. Tomai et al, to be published in Nuclear Fusion, 1987.

22. Taylor R.J. et al., Plasma Phys. and Contr. Nucl. Fusion Res. (1983) Vol. 3 (IAEA, Vienna, 1983) p.261.

23. TFR GROUP, Proc. 12th Europ. Conf. on Contr. Fusion and Plasma Phys., Vol. 9F, part II, p.108, Budapest (1985)

24. TRF GROUP, F Sand, Nucl. Fusion, Vol.25, No.12 (1985) p.1719.

TABLE I

	Dipole	Quadrupole
$\Delta[\,I\,Cr\,XXI/\langle n_e\rangle]/P_{RF}[a.u.]$	2.93	1.23
$\Delta\,[I\,Ni\,XXV/\langle n_e\rangle]/P_{RF}\,[a.u.]$	1.42	0.75
$\Delta\ P_{rad}/P_{RF}$	0.75	0.6
$\Delta\ Z_{eff}/P_{RF}\ [MW]^{-1}$	0.34	0.14
$\Delta\ \int n_e\,dl/P_{RF}\ [10^{13}\,m^{-2}\,W^{-1}]$	0.49	0.75
$\Delta\ \Sigma\,\phi_D^{TOT}/P_{RF}\ [10^{15}\,s^{-1}\,W^{-1}]$	0.05	0.58
τ_{INC}^{MAG} [sec]	0.12	0.16
τ_{INC}^{KIN} [sec]	0.17	0.23

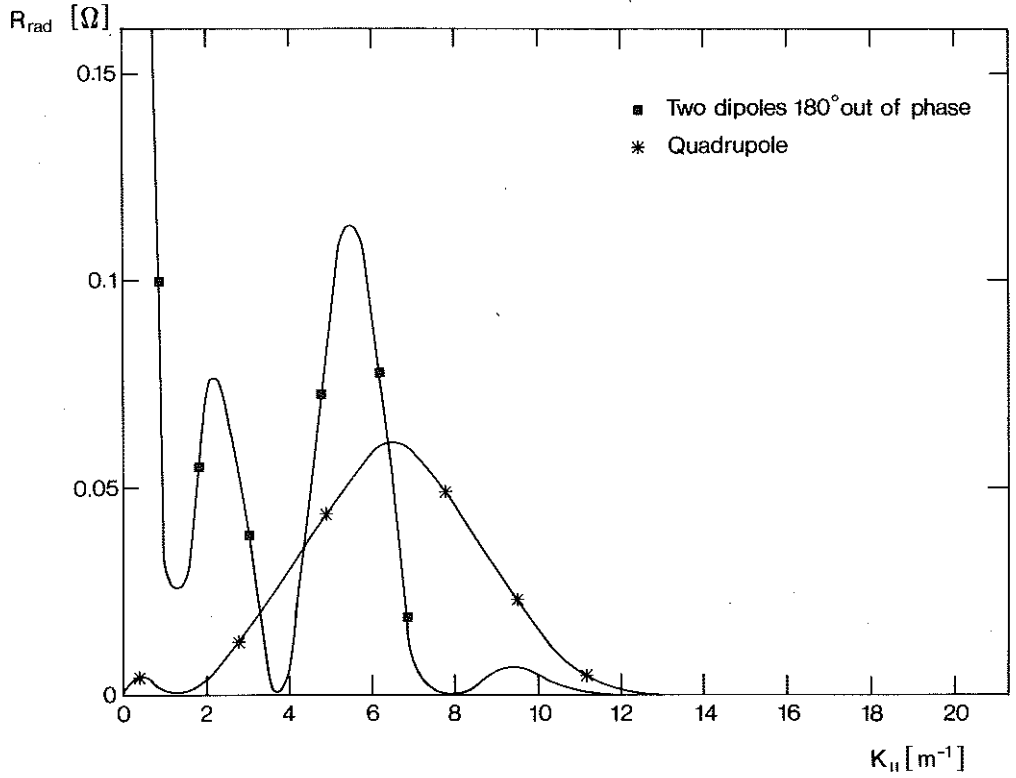

Fig. 1 Radiation resistance spectrum for the two dipole antennae 180° out of phase and for the quadrupole antenna. The contribution to the spectrum from the coaxial modes is included.

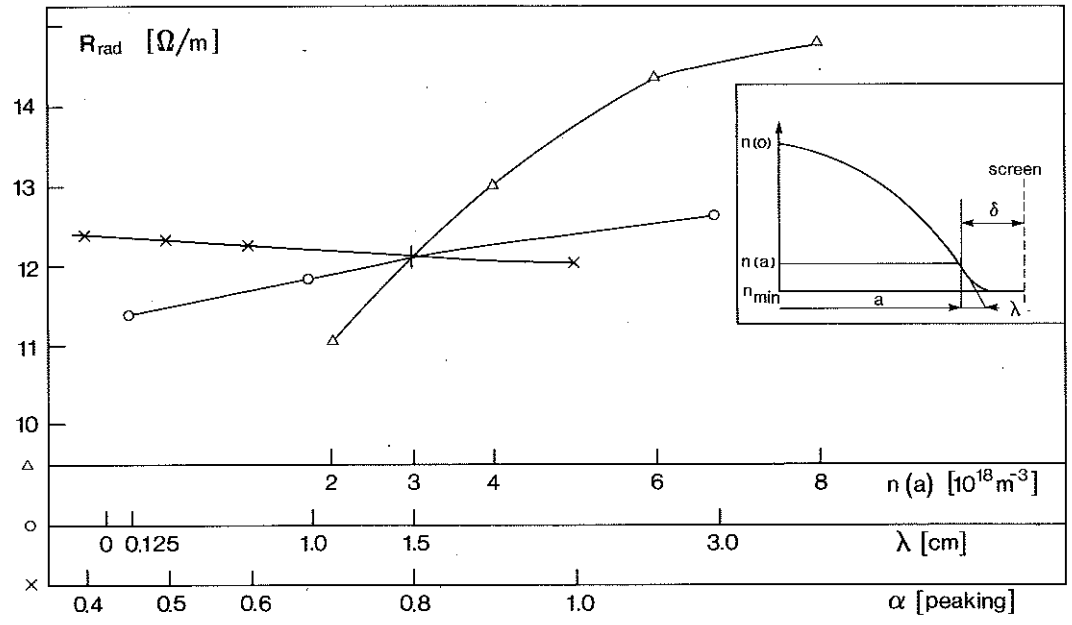

Fig. 2 Total radiation resistance of an antenna as a function of the density profile parameters as defined in the inset. α is the peaking factor, n(a) is the density at the last closed magnetic surface and λ is the characteristic scale length of the SOL density decay.

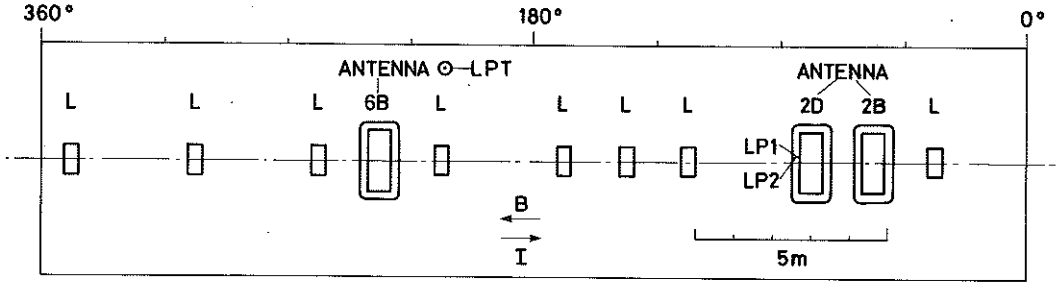

Fig. 3 A schematic drawing showing the unfolded JET torus. Positions of antennae within the torus. L denotes the carbon limiters. 2D and 2B denote the antennae being powered while 6B is the antenna used in the diagnostic mode. LP1 and LP2 are the Langmuir probes installed in the carbon tile of the 2D antenna while LPT is the probe inserted at the top of the vessel.

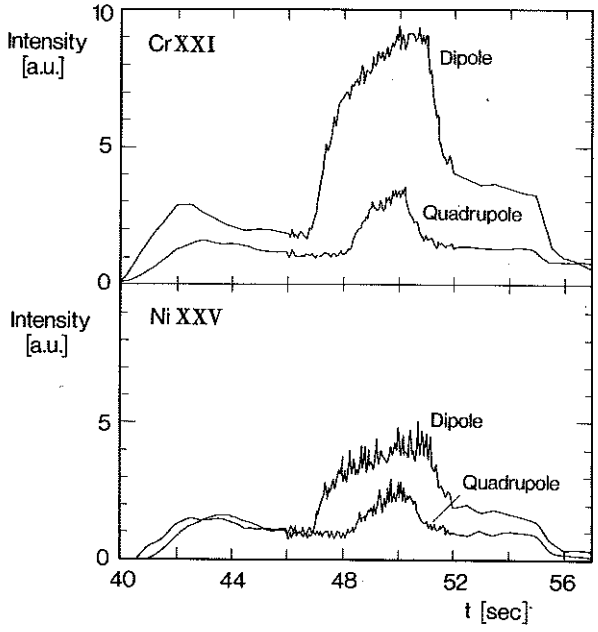

a) CrXXI and NiXXV lines

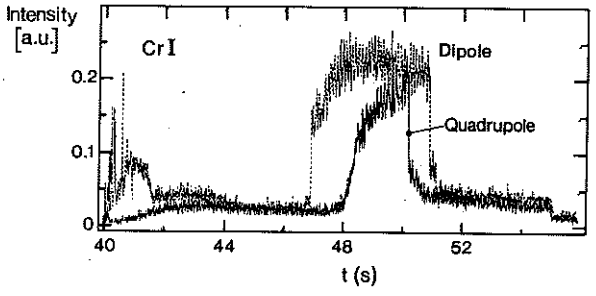

b) CrI line.

Fig. 4 Time evolution of the metal impurity lines in the cases of Dipole and Quadrupole configuration of the RF antennae. RF power coupled by quadrupoles was 1.3 MW while for dipole P_{RF} = 1.6 MW

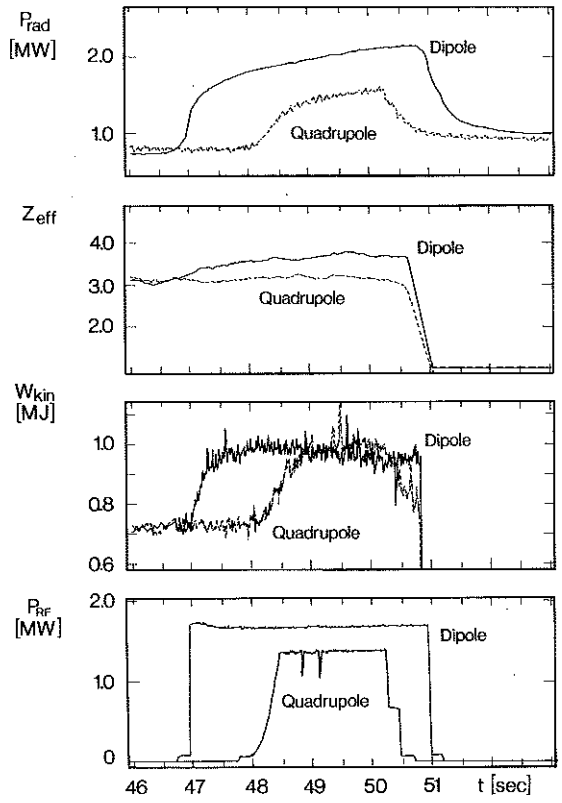

Fig. 5a) Time evolution of the total radiated power, Z_{eff} measured by visible bremstrahlung, the evolution of the total stored energy and the coupled RF power.

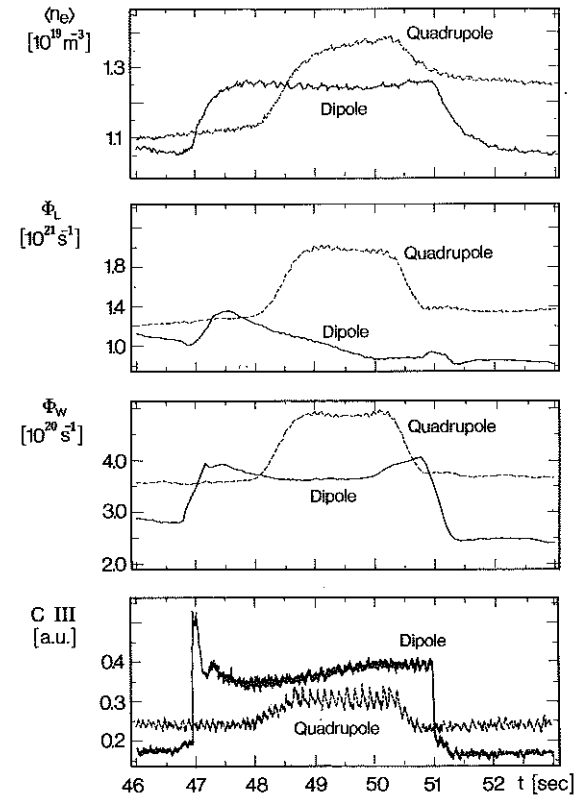

5b) Time evolution of the average plasma density, the limiter and wall neutral fluxes and the carbon flux from the vessel wall.

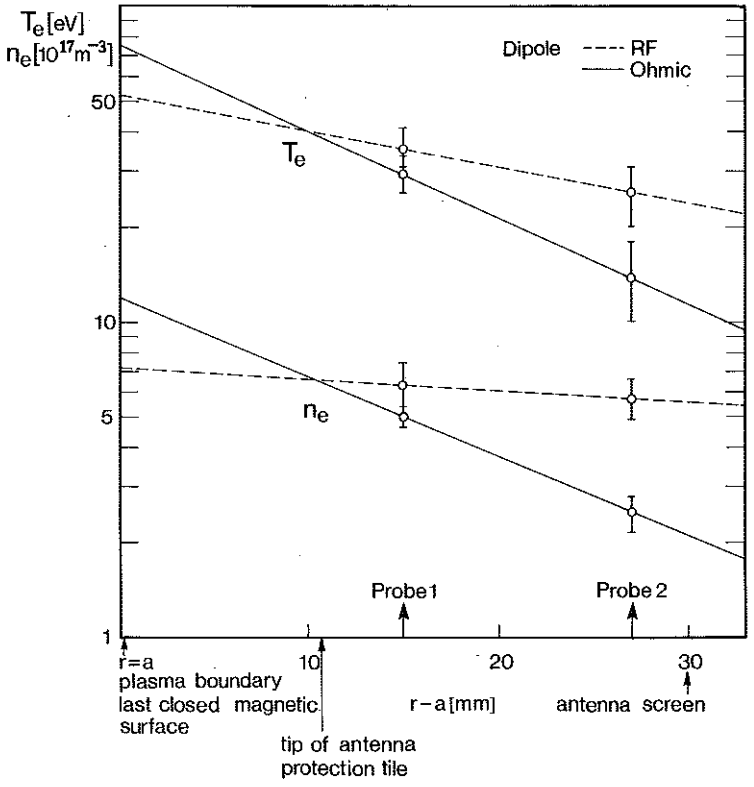

Fig. 6a) Steady-state electron density and temperature profile in the SOL in the ohmic and RF phase. Dipole configuration.

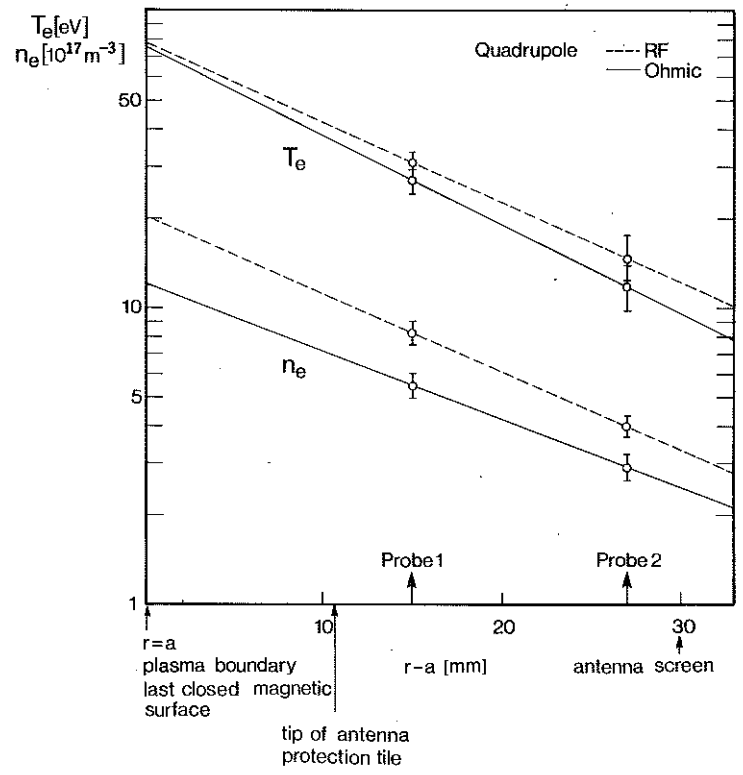

6b) Same as a) except Quadrupole configuration.

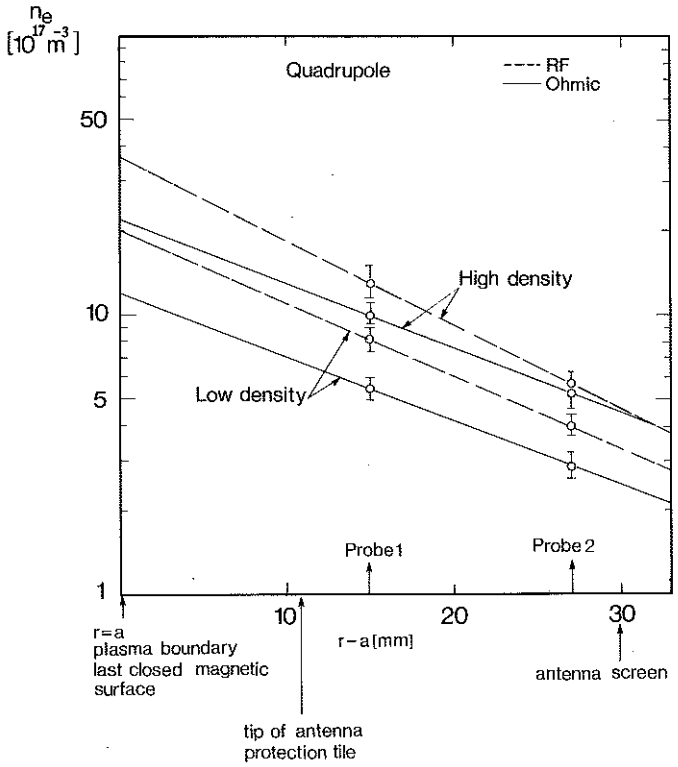

Fig. 7a) Steady-state density profiles in the SOL in the ohmic and RF phase for two different densities. Quadrupole configuration.

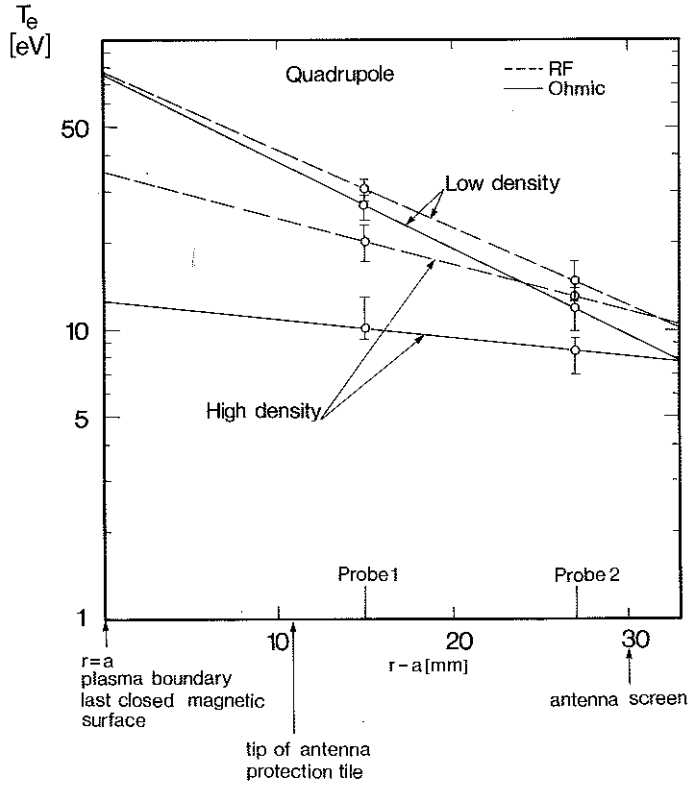

7b) Steady-state profile of the temperature in SOL for the same conditions as a).

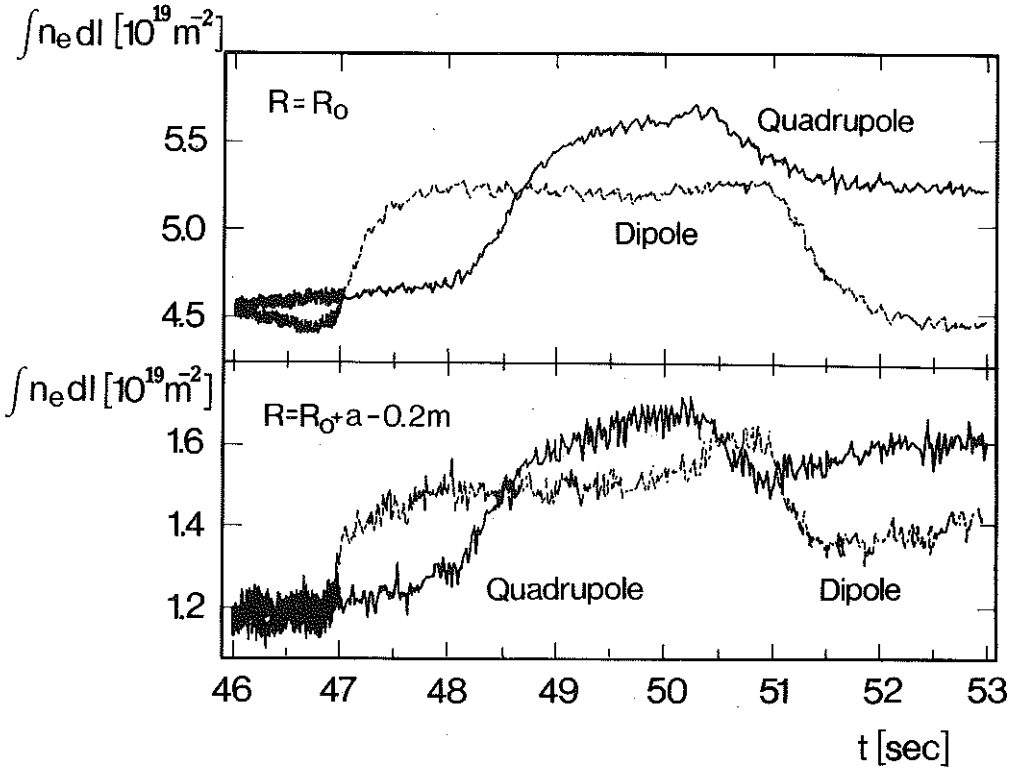

Fig. 8 Evolution of the line integral density measured along the vertical chord at two radial positions. At the centre and 23 cm from the antenna screen.

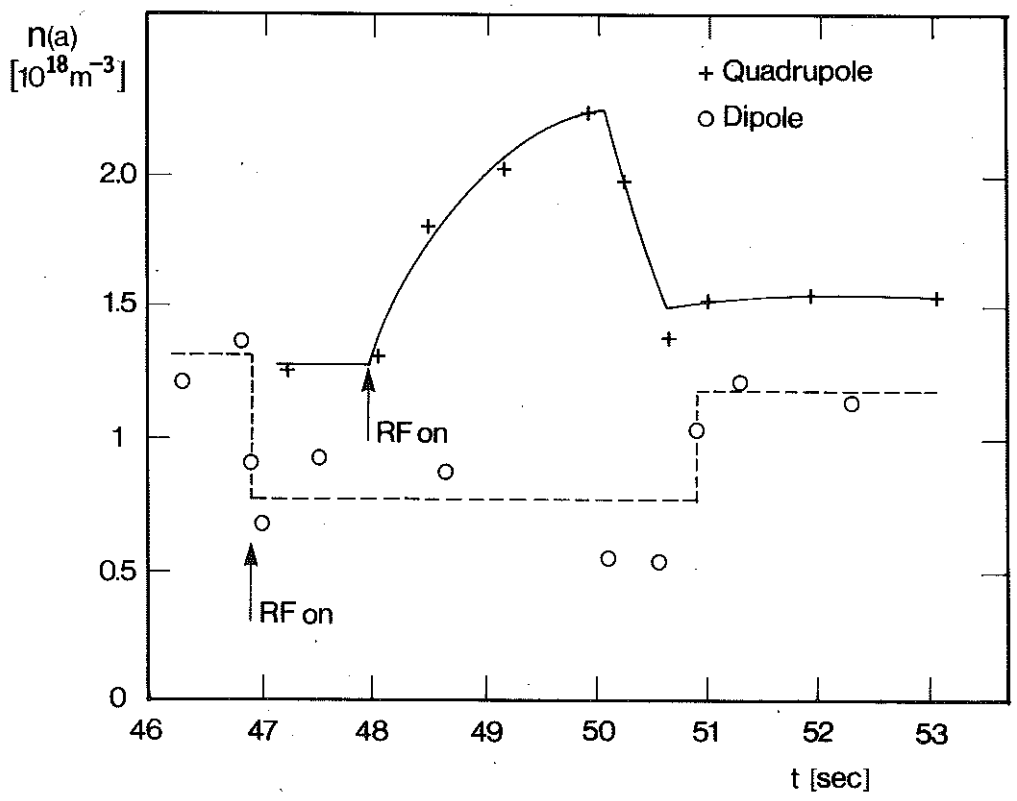

Fig. 9 Evolution of the edge density measured by the Langmuir probes during RF heating.

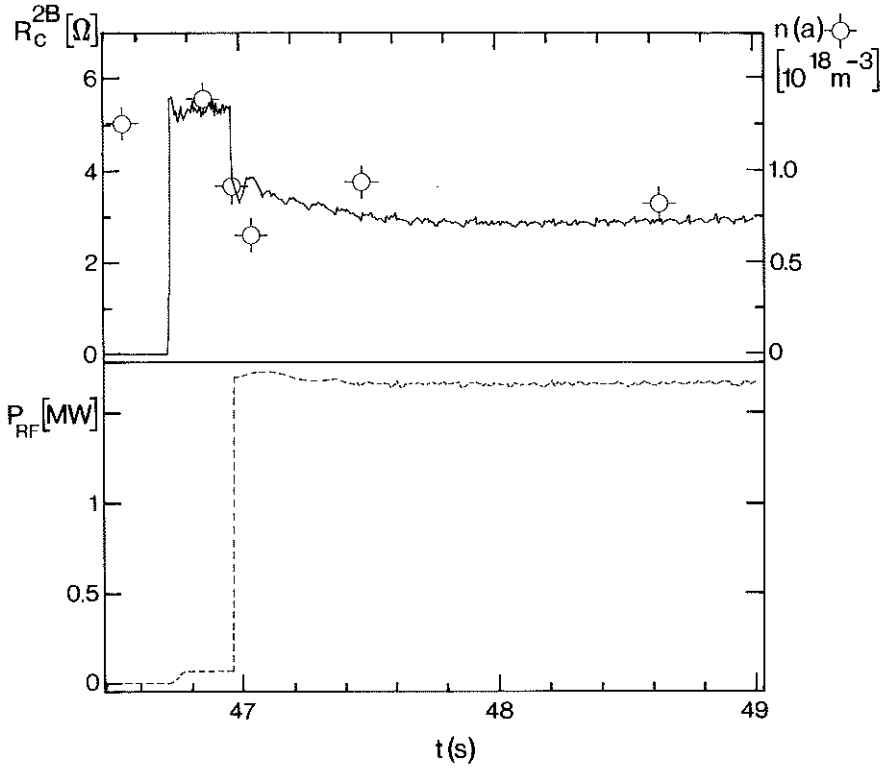

Fig.10 Coupling resistance, edge plasma density and the RF power during the dipole phasing.

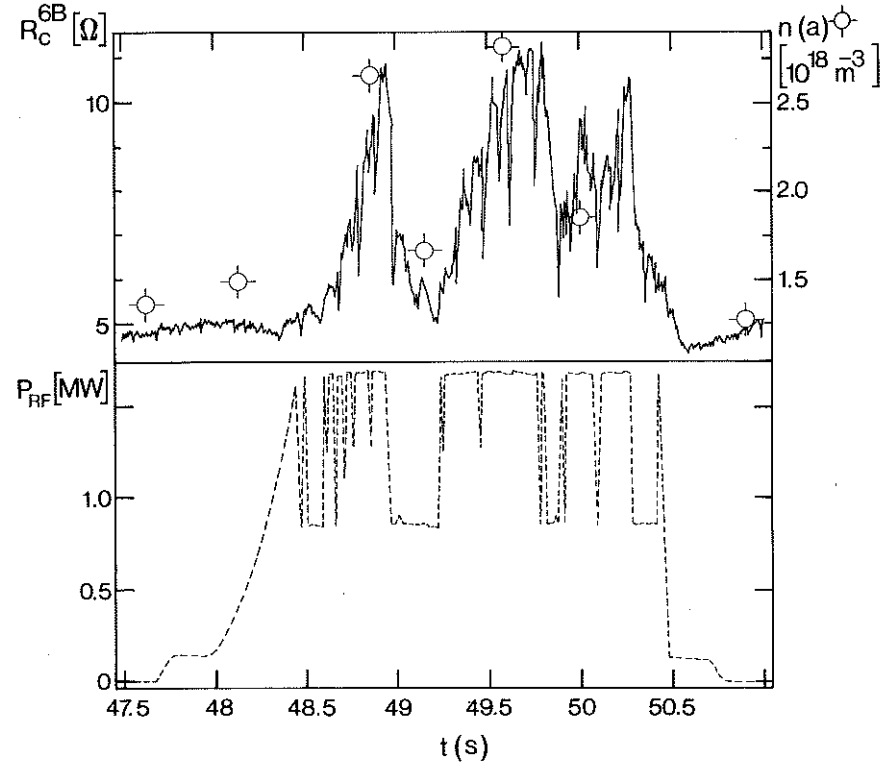

Fig.11 Coupling resistance, edge plasma density and the RF power pulse during the quadrupole phasing.

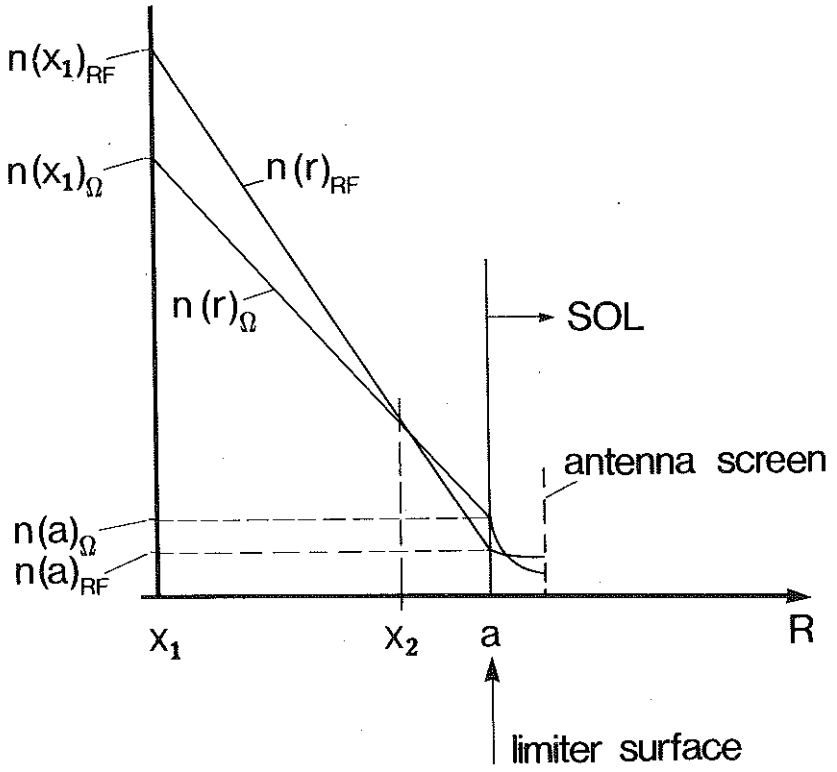

Fig.12 Detail of the density profiles close to the plasma edge in ohmic phase and during the RF heating with the dipole configuration.

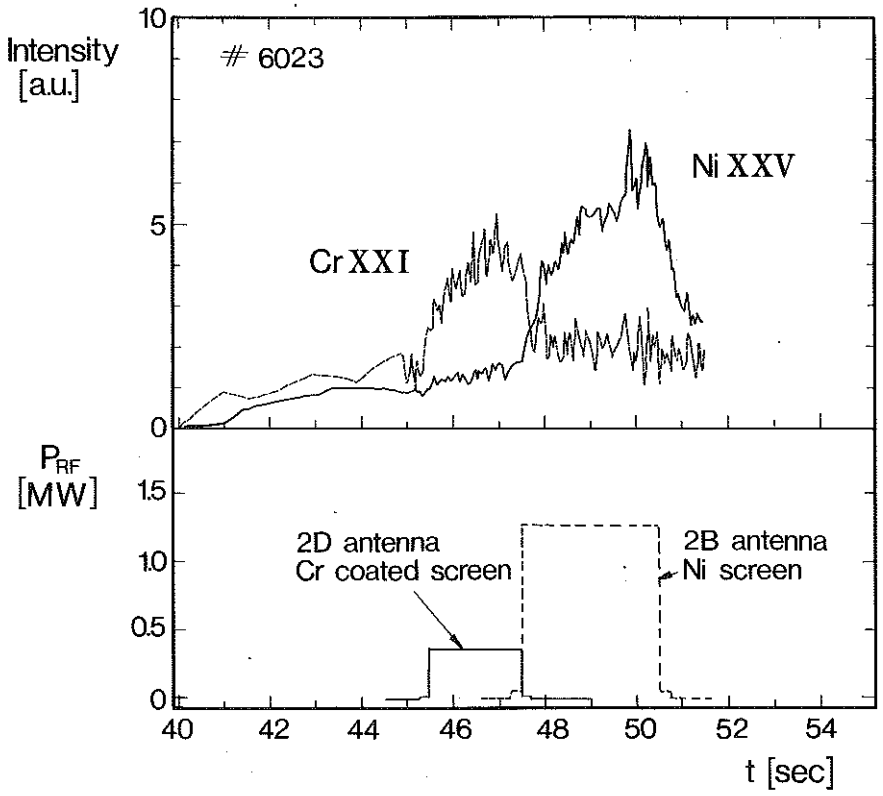

Fig.13 Time evolution of the CrXXI and NiXXV lines intensities as a function of the corresponding antenna activation.